Physics Letters B 775 (2017) 71–78

Contents lists available at ScienceDirect

Physics Letters B

www.elsevier.com/locate/physletb

Repulsive baryonic interactions and lattice QCD observables at imaginary chemical potential

Volodymyr Vovchenko [a,b,c,*], Attila Pásztor [d], Zoltán Fodor [d,e,f], Sandor D. Katz [e,g], Horst Stoecker [a,b,h]

[a] Institut für Theoretische Physik, Goethe Universität Frankfurt, Max-von-Laue-Str. 1, D-60438 Frankfurt am Main, Germany
[b] Frankfurt Institute for Advanced Studies, Giersch Science Center, Goethe Universität Frankfurt, Ruth-Moufang-Str. 1, D-60438 Frankfurt am Main, Germany
[c] Department of Physics, Taras Shevchenko National University of Kiev, Glushkova Ave 2, 03022 Kiev, Ukraine
[d] Department of Physics, Wuppertal University, Gaussstr. 20, D-42119 Wuppertal, Germany
[e] Institute for Theoretical Physics, Eötvös University, Pázmány P. sétány 1/A, H-1117 Budapest, Hungary
[f] Jülich Supercomputing Centre, Forschungszentrum Jülich, D-52425 Jülich, Germany
[g] MTA-ELTE "Lendület" Lattice Gauge Theory Research Group, Pázmány P. sétány 1/A, H-1117 Budapest, Hungary
[h] GSI Helmholtzzentrum für Schwerionenforschung GmbH, Planckstr. 1, D-64291 Darmstadt, Germany

ARTICLE INFO

Article history:
Received 18 August 2017
Received in revised form 4 October 2017
Accepted 19 October 2017
Available online 24 October 2017
Editor: W. Haxton

Keywords:
Hadron resonance gas
Excluded volume
Imaginary chemical potential

ABSTRACT

The first principle lattice QCD methods allow to calculate the thermodynamic observables at finite temperature and imaginary chemical potential. These can be compared to the predictions of various phenomenological models. We argue that Fourier coefficients with respect to imaginary baryochemical potential are sensitive to modeling of baryonic interactions. As a first application of this sensitivity, we consider the hadron resonance gas (HRG) model with repulsive baryonic interactions, which are modeled by means of the excluded volume correction. The Fourier coefficients of the imaginary part of the net-baryon density at imaginary baryochemical potential – corresponding to the fugacity or virial expansion at real chemical potential – are calculated within this model, and compared with the $N_t = 12$ lattice data. The lattice QCD behavior of the first four Fourier coefficients up to $T \simeq 185$ MeV is described fairly well by an interacting HRG with a single baryon–baryon eigenvolume interaction parameter $b \simeq 1$ fm^3, while the available lattice data on the difference $\chi_2^B - \chi_4^B$ of baryon number susceptibilities is reproduced up to $T \simeq 175$ MeV.

© 2017 The Authors. Published by Elsevier B.V. This is an open access article under the CC BY license (http://creativecommons.org/licenses/by/4.0/). Funded by SCOAP^3.

1. Introduction

The Monte Carlo lattice QCD simulations provide the equation of state of the $(2 + 1)$-flavor strongly interacting matter at zero chemical potential [1–3]. A crossover-type transition is observed [4]. The pseudocritical temperature T_{pc} of the transition depends on the observable used to define it, estimates based on chiral condensate and its susceptibility give $T_{pc} \approx 155$ MeV [5,6], while observables based on strangeness suggest somewhat higher temperatures [5,7]. Below the transition one expects to find the confined hadronic phase. Many lattice QCD observables in that temperature range are indeed well described by a simple ideal hadron resonance gas (HRG) model [7–10].

It was pointed out recently, that the behavior of lattice observables in the crossover region, particularly of correlations and fluctuations of conserved charges, is very sensitive to the modeling of the baryonic interactions [11,12]. This sensitivity is of great interest, since hadronic modeling of conserved charge fluctuations is often used to extract freeze-out parameters of heavy ion collisions [13,14]. Lattice observables at finite net baryon density can certainly be expected to be even more sensitive to the modeling of these interactions. Unfortunately, direct Monte Carlo calculations at finite μ_B are hindered by the sign problem. Main methods to circumvent this problem include the reweighting techniques [15–18], the Taylor expansion around $\mu = 0$ [19–22], and the analytic continuation from imaginary μ [23–31]. These methods have allowed to calculate some thermodynamic features of QCD at small but finite chemical potentials [32–34].

In the present work we consider the imaginary μ method. We use the updated version of the lattice data, shown previously in Ref. [35]. However, instead of performing analytic continuation from imaginary chemical potential to real chemical potential, we instead directly compare lattice data at imaginary μ to the

* Corresponding author.
E-mail address: vovchenko@fias.uni-frankfurt.de (V. Vovchenko).

https://doi.org/10.1016/j.physletb.2017.10.042
0370-2693/© 2017 The Authors. Published by Elsevier B.V. This is an open access article under the CC BY license (http://creativecommons.org/licenses/by/4.0/). Funded by SCOAP^3.

corresponding predictions of the phenomenological models. Some phenomenological models were considered at imaginary chemical potential before, such as the quasiparticle model [36] or the PQM model [37]. Comparison of phenomenological models with lattice simulations at imaginary μ was considered in [24,38–40]. In the present work, our focus is on the HRG model with repulsive interactions for baryon–baryon and antibaryon–antibaryon pairs, modeled by means of the excluded volume (EV) correction.

The paper is organized as follows: in Sec. 2 the lattice observables at imaginary baryochemical potential, which are studied in the present work, are introduced. Sec. 3 lists the predictions for these observables from several phenomenological models. The lattice method is described in Sec. 4, and in Sec. 5 lattice results are compared to the predictions of interacting HRG models. Summary in Sec. 6 closes the article.

2. QCD observables at imaginary baryochemical potential

Due to the baryon–antibaryon symmetry, the QCD pressure is an even function of a real baryochemical potential μ_B at a finite temperature. This quantity can then be written as the following series expansion:

$$\frac{p(T,\mu_B)}{T^4} = \sum_{k=0}^{\infty} p_k(T)\,\cosh(k\,\mu_B/T), \tag{1}$$

provided that the expansion is convergent at a given T-μ_B pair.[1] At $\mu_B = 0$, the pressure is simply the sum of all coefficients $p_k(T)$. Therefore these can be interpreted as the partial pressures, coming from the sectors of the Hilbert space with a different baryon number.

The first-order net baryon susceptibility $\chi_1^B(T,\mu_B) \equiv \partial(p/T^4)/\partial(\mu_B/T)$ is proportional to the net baryon density and it is equal to

$$\chi_1^B(T,\mu_B) = \frac{\rho_B(T,\mu_B)}{T^3} = \sum_{k=1}^{\infty} b_k(T)\,\sinh(k\,\mu_B/T), \tag{2}$$

where, by definition,

$$b_k(T) \equiv k\,p_k(T). \tag{3}$$

It is clear that the knowledge of all $p_k(T)$ coefficients provides complete information about the thermodynamic properties of QCD in the region of the phase diagram where the series expansion given by Eq. (1) is convergent.

One can consider the susceptibility χ_1^B in Eq. (2) at a purely imaginary value of the baryochemical potential, i.e. at $\mu_B = i\,\tilde{\mu}_B$. The analytic continuation yields

$$\chi_1^B(T,i\tilde{\mu}_B) = i\sum_{k=1}^{\infty} b_k(T)\,\sin(k\,\tilde{\mu}_B/T), \tag{4}$$

i.e. χ_1^B itself becomes purely imaginary. The imaginary part of χ_1^B in Eq. (4) has explicit form of the trigonometric series expansion, with $b_k(T)$ being the corresponding temperature dependent Fourier coefficients. If the $\tilde{\mu}_B$-dependence of χ_1^B is known (e.g. from lattice simulations), then the coefficients $b_k(T)$ can be calculated in the standard way:

$$b_k(T) = \frac{2}{\pi}\int_0^{\pi} d\tilde{\mu}_B\,[\mathrm{Im}\,\chi_1^B(T,i\tilde{\mu}_B)]\,\sin(k\,\tilde{\mu}_B/T). \tag{5}$$

[1] Throughout this work we assume that strangeness and electric charge chemical potentials are zero, i.e. $\mu_S = \mu_Q = 0$.

3. Phenomenological models

In some analytic models of the equation of state, the coefficients $b_k(T)$ can be worked out explicitly.

3.1. Ideal HRG

A popular model to describe the confined phase of QCD at low temperatures is the hadron resonance gas model. In its simplest implementation, the system is modeled as a non-interacting mixture of all known hadrons and resonances. It is argued [41], that the inclusion into the model of all known resonances as free non-interacting (point-like) particles, may allow for an effective modeling of the attractive interactions between hadrons, including the formation of narrow resonances and of Hagedorn states. This ideal HRG model has a long history of being used to describe the hadron production in heavy-ion collisions at various collision energies [42–46].

In the present HRG analysis we employ the Boltzmann approximation for all baryons. This is a good approximation for the observables of interest. We do not include the light nuclei into the HRG particle list. The inclusion of nuclei would induce nonzero $b_2, b_3, \ldots$, but always with a positive sign. This is in contrast to our lattice results, e.g. that $b_2 < 0$, indicating that the next important correction to the HRG model is not from these states, but from repulsive interactions. The net baryon density ρ_B^{id} in the ideal HRG model reads

$$\rho_B^{\mathrm{id}}(T,\mu_B) = 2\,\phi_B(T)\,\sinh(\mu_B/T), \tag{6}$$

where

$$\phi_B(T) = \sum_{i\in B}\int dm\,\rho_i(m)\,\frac{d_i\,m^2\,T}{2\pi^2}\,K_2\left(\frac{m}{T}\right) \tag{7}$$

is the baryonic spectrum, with d_i and ρ_i being, respectively, the degeneracy and a properly normalized mass distribution for hadron type i, and where the sum goes over all baryons in the system. Note that the summation does not include antibaryons. We include the baryon states, which are listed in the Particle Data Tables [47] and have a confirmed status there. The function ρ_i takes into account the non-zero widths of the resonances by the additional integration over their Breit–Wigner shapes, following Refs. [48,49].

It is evident from Eq. (6) that all Fourier coefficients b_k^{id} are equal to zero for $k \geq 2$. For the first coefficient one obtains $b_1^{\mathrm{id}}(T) = 2\,\phi_B(T)/T^3$.

3.2. HRG with repulsive baryonic interactions

In a more realistic HRG model one has to also take into account the attractive and repulsive interactions between hadrons which cannot be attributed to the resonance formation. In particular, the nucleon–nucleon interaction is known to be largely repulsive at short distances and the corresponding scattering phase shifts are not known to exhibit any resonance structure. The importance of the van der Waals like interactions between baryons for lattice QCD observables was recently pointed out in Ref. [11]. In the present work we perform similar analysis for the observables at imaginary chemical potential. To keep things simple, we focus on the short-range repulsion between baryons.

Following Refs. [11,50] we assume that repulsive interactions exist between all baryon–baryon and antibaryon–antibaryon pairs. These interactions are modeled by means of the excluded-volume (EV) correction [51]. At the same time, the EV interactions between all other hadron pairs are explicitly omitted. It is not clearly established whether significant EV-type interactions exist between

hadron pairs other than (anti)baryons (see Ref. [11] for discussion). We denote this setup as the EV-HRG model. Note that this model is quite different from the usual EV prescription used in HRG model analysis: normally it is assumed that all hadrons, including mesons, have identical eigenvolume, and, thus, all hadron pairs interact repulsively at short distances [52–54]. However, a presence of a significant mesonic eigenvolume leads to a notable suppression of thermodynamic functions at $\mu = 0$, which appears to be at odds with the lattice data [55,56]. Note that EV corrections were recently considered also for a glueball gas in Yang–Mills theory, in the context of the corresponding lattice data [57].

The EV-HRG model consists of three independent sub-systems: Non-interacting mesons, interacting baryons, and interacting antibaryons. The (anti)baryonic partial pressure $p^{\rm ev}_{B(\bar{B})}$ satisfies the transcendental equation $p^{\rm ev}_{B(\bar{B})}(T,\mu_B) = p^{\rm id}_{B(\bar{B})}(T,\mu_B - b\,p^{\rm ev}_{B\bar{B}})$, which can be written in the Boltzmann approximation as follows:

$$p^{\rm ev}_{B(\bar{B})}(T,\mu_B) \;=\; T\,\phi_B(T)\,\exp\left(\frac{\mu_B - b\,p^{\rm ev}_{B(\bar{B})}}{T}\right). \tag{8}$$

Let us denote the total densities of baryons and of antibaryons as $n^{\rm ev}_B \equiv (\partial\, p^{\rm ev}_B/\partial\,\mu_B)_T$ and $n^{\rm ev}_{\bar{B}} \equiv -(\partial\, p^{\rm ev}_{\bar{B}}/\partial\,\mu_B)_T$, respectively. By definition, the net baryon density is then $\rho^{\rm ev}_B = n^{\rm ev}_B - n^{\rm ev}_{\bar{B}}$. In the Boltzmann approximation one has the following transcendental equations for $n^{\rm ev}_B$ and $n^{\rm ev}_{\bar{B}}$ [11]

$$n^{\rm ev}_B = (1 - b\,n^{\rm ev}_B)\,\lambda_B\,\phi_B(T)\,\exp\left(-\frac{b\,n^{\rm ev}_B}{1 - b\,n^{\rm ev}_B}\right), \tag{9}$$

$$n^{\rm ev}_{\bar{B}} = (1 - b\,n^{\rm ev}_{\bar{B}})\,\lambda_B^{-1}\,\phi_B(T)\,\exp\left(-\frac{b\,n^{\rm ev}_{\bar{B}}}{1 - b\,n^{\rm ev}_{\bar{B}}}\right), \tag{10}$$

with $\lambda_B \equiv e^{\mu_B/T}$. Let us assume n_B and $n_{\bar{B}}$ in the following fugacity expansion form:

$$\frac{n^{\rm ev}_B}{T^3} = \frac{1}{2}\sum_{k=1}^{\infty} b^{\rm ev}_k(T)\,\lambda_B^k, \tag{11}$$

$$\frac{n^{\rm ev}_{\bar{B}}}{T^3} = \frac{1}{2}\sum_{k=1}^{\infty} b^{\rm ev}_k(T)\,\lambda_B^{-k}. \tag{12}$$

The prefactor 1/2 is chosen such that the corresponding fugacity expansion for the net baryon density $\rho^{\rm ev}_B \equiv n^{\rm ev}_B - n^{\rm ev}_{\bar{B}}$ coincides with Eq. (2).

Putting this into Eq. (9) and truncating at the fourth power of λ_B one obtains analytic expressions for $b^{\rm ev}_k$:

$$b^{\rm ev}_1(T) = 2\,\frac{\phi_B(T)}{T^3}, \tag{13}$$

$$b^{\rm ev}_2(T) = -4\,[b\phi_B(T)]\,\frac{\phi_B(T)}{T^3}, \tag{14}$$

$$b^{\rm ev}_3(T) = 9\,[b\,\phi_B(T)]^2\,\frac{\phi_B(T)}{T^3}, \tag{15}$$

$$b^{\rm ev}_4(T) = -\frac{64}{3}\,[b\,\phi_B(T)]^3\,\frac{\phi_B(T)}{T^3}. \tag{16}$$

The first coefficient, $b^{\rm ev}_1(T)$, coincides with the ideal HRG model result. Thus, it is unaffected by the baryon–baryon EV interactions.[2] Contrary to the ideal HRG model, the higher-order coefficients are non-zero. They seem to follow a generic pattern: even order coefficients are negative while odd order coefficients are positive. This sign-changing pattern was verified to be present in the EV-HRG model at least up to the 10th order. As seen from Eqs. (13)–(16), the coefficients scale with the eigenvolume parameter as $b^{\rm ev}_k \propto b^{k-1}$. The ratios $b^{\rm ev}_k/\left(b^{\rm ev}_1\right)^k$ scale as $(-1)^{k+1}(bT^3)^{k-1}$, meaning that more and more Fourier coefficients become non-negligible as the temperature is increased.

One may also consider a more general case, where both the repulsive and also the attractive van der Waals (vdW) interactions between baryons are present. For this vdW-HRG model [11] the coefficients $b_k(T)$ can also be calculated analytically. The details are given in Appendix.

3.3. High-temperature limit of massless quarks and gluons

Let us also mention the high-temperature limit, where the thermodynamic features of QCD are expected to resemble those of a massless ideal gas of quarks and gluons. In this Stefan–Boltzmann (SB) limit the pressure is

$$\frac{p^{\rm SB}}{T^4} = \frac{8\pi^2}{45} + \sum_{f=u,d,s}\left[\frac{7\pi^2}{60} + \frac{1}{2}\left(\frac{\mu_f}{T}\right)^2 + \frac{1}{4\pi^2}\left(\frac{\mu_f}{T}\right)^4\right]. \tag{17}$$

Since we only consider the case $\mu_S = \mu_Q = 0$, one has $\mu_f = \mu_B/3$. The net baryon susceptibility at imaginary μ_B reads

$$\chi_1^B(T, i\tilde{\mu}_B) = \left.\frac{\partial(p/T^4)}{\partial(\mu_B/T)}\right|_{\mu_B = i\,\tilde{\mu}_B} = \frac{i}{3}\left[\frac{\tilde{\mu}_B}{T} - \frac{1}{9\pi^2}\left(\frac{\tilde{\mu}_B}{T}\right)^3\right]. \tag{18}$$

At high temperatures, Roberge–Weiss transition is expected at $\tilde{\mu}_B = \pi\,T$ [58]. Thus, the polynomial behavior given by Eq. (18) should only be considered up to this imaginary chemical potential value.

The coefficients $b^{\rm SB}_k$ are calculated according to Eq. (5). One obtains:

$$b^{\rm SB}_k = \frac{(-1)^{k+1}}{k}\,\frac{4\,[3 + 4\,(\pi k)^2]}{27\,(\pi k)^2}. \tag{19}$$

The Fourier coefficients at very high temperatures show a sign structure: even coefficients are negative, odd coefficients are positive. This is exactly the same sign structure as predicted by the EV-HRG model. On the other hand, as opposed to the strong temperature dependence in the ratios predicted by the EV-HRG model, namely $b^{\rm ev}_k/\left(b^{\rm ev}_1\right)^k \propto (-1)^{k+1}(bT^3)^{k-1}$, in the free quark limit this ratio is temperature independent.

4. Lattice method

Our lattice simulations use the tree-level Symanzik improved gauge action and 2+1+1 flavors of four times stout smeared staggered quarks, with the smearing parameter $\rho = 0.125$. The same 4stout lattice setup was also used in [10,31–33,59]. We use physical quark masses. The details of the lattice action can be found in [10]. We generate configurations with Im $\mu_B > 0$, in the temperature range $135 \le T \le 230$ MeV. The geometry of our lattices is $48^3 \times 12$. A continuum extrapolation was not attempted so far. We run roughly 1000–2000 configurations at each simulation point, separated by 10 HMC trajectories. We measure the imaginary part χ_1^B on the lattices, and carry out a discrete Fourier transform to obtain the observables b_1, b_2, b_3 and b_4. The errors on the lattice data points are purely statistical, calculated from 48 jackknife samples.

The crucial observation is that the Fourier coefficients at imaginary chemical potential correspond to partial pressures coming

[2] Note, however, that $b_1(T)$ are potentially affected by the meson-baryon EV-type interactions, which are not considered in the present work.

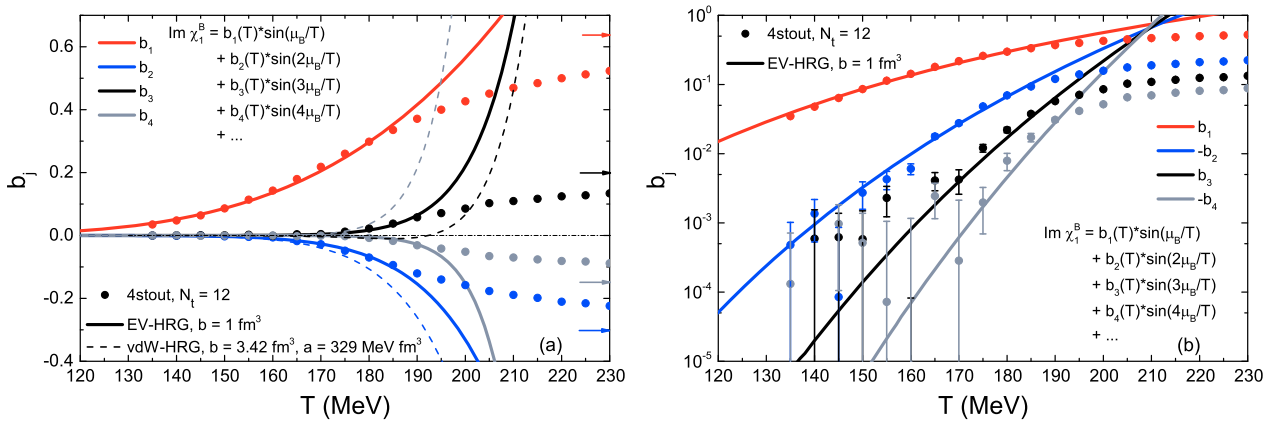


Fig. 1. The temperature dependence of the first four Fourier coefficients b_k (4), calculated on the lattice with the 4stout, $N_t = 12$ setup (symbols), and within the EV-HRG model with baryonic eigenvolume parameter $b = 1$ fm^3 (solid lines). This dependence is shown on (a) the linear and (b) the logarithmic scales. The dashed lines in (a) show the calculations within the vdW-HRG model, with van der Waals parameters a and b fixed by the properties of the nuclear ground state [11]. The arrows in (a) correspond to the Stefan–Boltzmann limit (19) of the massless gas of quarks and gluons.

from different sectors of the Hilbert space. These can also be identified with the fugacity or relativistic virial expansion coefficients for real chemical potential. From a phenomenological point of view, this makes the Fourier coefficients particularly sensitive to the details of hadronic models. This was pointed out in [31], where the different strangeness sectors of the theory were separated, and later used to constrain the hadronic spectrum in the context of the ideal HRG model. Note that the fugacity expansion of the logarithm of the partition function, log Z, employed in the present work, is quite different from the fugacity expansion of the fermion determinant, which corresponds to the fugacity expansion of Z and which had also been used in some lattice studies [60,61]. Strong finite volume scaling effects in the fugacity expansion of log Z are not expected, in contrast to the fugacity expansion of Z.

Other studies [62] exploit the connection of the virial coefficients to the fluctuations of conserved charges at $\mu = 0$. E.g., if one neglects the third and higher order coefficients in the expansion (1), i.e. $a_3 = a_4 = \cdots = 0$, then the difference $\chi_4^B - \chi_2^B$ of the fourth and second order baryon susceptibilities is simply proportional to the second coefficient a_2. The validity of the truncation to only the second coefficient breaks down as the temperature is increased, and such a method no longer works correctly. In this work we use a different approach, and calculate the expansion coefficients directly, by exploiting the fact that they become Fourier coefficients at an imaginary chemical potential. This allows us to consider the higher order coefficients as well, apart from b_2. Moreover, in [31] we show by explicit lattice calculations of the strangeness sectors in the confined phase, that in the cases where the truncation of the virial expansion is warranted, and the two methods should agree, our method produces smaller statistical errors for the same computational cost. We note that coefficients b_k were considered in the lattice studies before (see e.g. Refs. [40, 63–65]), where they were estimated by fitting the lattice data with the truncated fugacity expansion.

5. Results and discussion

5.1. Hadronic description

Fig. 1 depicts the temperature dependence of the first four Fourier coefficients b_k (4), calculated on the lattice with the 4stout, $N_t = 12$ setup (symbols), and within the EV-HRG model with baryonic eigenvolume parameter $b = 1$ fm^3 (solid lines). This dependence is shown (a) on the linear scale, and (b) on the logarithmic scale.

As mentioned above, the b_1 coefficient is not affected by the baryon–baryon interactions. Its behavior in the EV-HRG model is the same as in the ideal HRG model, and it is determined solely by the input particle list and, less so, by the modeling of the finite resonance widths. The HRG model with the PDG-based hadron list, employed in the present work, stays rather close to the lattice data for b_1 up to $T \simeq 185$ MeV, but does not reproduce the inflection, and therefore does not describe the temperature derivative of the $b_1(T)$ curve well from $T \simeq 175$ MeV.

Lattice calculations predict non-zero values for the higher-order coefficients. For instance, the second coefficient b_2 is negative in the considered temperature range. As seen from Fig. 1(a), this coefficient starts to notably deviate from zero at about $T \simeq 160$ MeV. This deviation signals the end of the applicability range of the ideal HRG model, which predicts $b_2 \equiv 0$ at all temperatures.

The negative sign is expected in the case where the second Fourier coefficient is dominated by the elastic two-to-two baryon–baryon scattering with a repulsive interaction. In this case the second Fourier coefficient is given by the Beth–Uhlenbeck formula [41,66], and its sign is therefore given by the sign of the energy derivative of the scattering phase shift, which is negative in the case of a repulsive interaction.

The third and fourth order coefficients, as calculated on the lattice, start to notably deviate from zero at successively higher temperatures. Lattice calculations show a peculiar alternating sign hierarchy: odd order coefficients, b_1 and b_3, are positive while the even order coefficients, b_2 and b_4, are negative.[3] We note that indications for such behavior of the first four coefficients were already seen in lattice simulations before [40,63–65], and, in particular, the alternating sign structure of the first four coefficients was obtained in Ref. [40]. Interestingly, this structure is also predicted by the EV-HRG model with repulsive baryonic interactions, as seen in Eqs. (13)–(16). In fact, the EV-HRG model with appropriately chosen baryonic eigenvolume parameter describes the lattice data fairly well: as seen in Fig. 1, all four coefficients calculated in the EV-HRG model with $b = 1$ fm^3 are in good agreement with the lattice data at temperatures $T \lesssim 185$ MeV. Thus, such a choice of the b value includes many of the non-perturbative corrections, which are otherwise very complicated. The lattice results for b_k do contain the inflection points in the temperature dependence, which are not predicted by the EV-HRG model. All four coefficients, as

[3] This proliferation of Fourier coefficients at high temperature can also be regarded as a signal for the Roberge–Weiss transition [58].

calculated on the lattice, appear to converge slowly towards the corresponding Stefan–Boltzmann limiting values, which are given by Eq. (19).

For completeness, we also depict the results obtained within the vdW-HRG model [11], with vdW parameters a and b extracted from the nuclear ground state properties. Unlike EV-HRG model, this model describes correctly the basic binding properties of nuclear matter at low temperatures and high baryochemical potentials, and it has no free parameters which can be adjusted to fit lattice data. The vdW-HRG model gives a fair description of b_2 at lower temperatures, but misses the b_3 and b_4. It appears that nuclear matter based values of vdW parameters, namely $a = 329$ MeV fm^3 and $b = 3.42$ fm^3, are overestimated when applied to the description of the lattice data at $T = 130$–190 MeV. The EV-HRG model with a smaller $b = 1$ fm^3 does a much better job in describing the lattice data. It would be interesting to reconcile both models, and obtain a simultaneous description of the lattice data and of the nuclear matter properties.

The Fourier expansion coefficients $b_k(T)$ can be contrasted with the net baryon number susceptibilities $\chi_k^B(T)$ at zero baryochemical potential, which are defined as follows:

$$\chi_k^B(T) \equiv \left.\frac{\partial^k (p/T^4)}{\partial (\mu_B/T)^k}\right|_{\mu_B=0} . \tag{20}$$

χ_k^B are proportional to the coefficients of the Taylor expansion of the QCD pressure with respect to μ_B, they correspond to the cumulants of the baryon number distribution at a given temperature and, therefore, they are more directly connected to the observables which are measured in heavy-ion collision experiments. It is particularly instructive to consider the difference $\chi_2^B - \chi_4^B$. The fugacity expansion (2) for this quantity reads

$$\chi_2^B - \chi_4^B = -\sum_{k=2}^{\infty} k\,(k^2-1)\,b_k(T)\,. \tag{21}$$

In the ideal HRG this quantity is strictly zero. This is no longer the case when baryonic interactions are included. When the effects of baryon–baryon interactions are small, the third and higher order coefficients in Eq. (21) can be neglected. In this case $\chi_2^B - \chi_4^B$ is directly proportional to b_2, which is in turn proportional to the second virial coefficient of baryon–baryon interactions. This fact was exploited in Ref. [62]. When the total density of baryons is high, however, higher order terms of the expansion (21) have to be considered as well.

We calculate the temperature dependence of the difference $\chi_2^B - \chi_4^B$ using the EV-HRG model with $b = 1$ fm^3. To study the breakdown of the truncated fugacity expansion at high temperatures, we consider the expansion (21), which is truncated at the second, third, or fourth order. It is calculated using Eqs. (14)–(16) for the b_k coefficients in the EV-HRG model. These calculations are compared with the full, untruncated result, obtained by directly solving the transcendental equation (8) for the pressure and using the definition (20) for χ_k^B. Lattice QCD results from Refs. [10] and [34,67] are also shown.

Results exhibited in Fig. 2 demonstrate the validity range for the different orders of truncation used for calculating $\chi_2^B - \chi_4^B$. The second order works well up to $T \simeq 150$ MeV, the third order is applicable up to $T \simeq 160$ MeV, and the fourth order reproduces the full result until $T \simeq 170$ MeV. We note that the validity range of a particular truncation scheme can be different if used for a different observable. Our above conclusions apply specifically to $\chi_2^B - \chi_4^B$.

As seen from Fig. 2, the full EV-HRG model reproduces the lattice data quite well up to $T \simeq 175$ MeV. The non-zero values

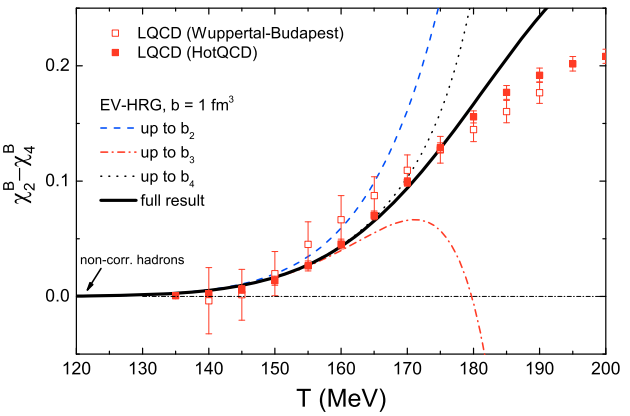


Fig. 2. The temperature dependence of $\chi_2^B - \chi_4^B$, calculated within the EV-HRG model with baryonic eigenvolume parameter $b = 1$ fm^3 (solid line). Other lines depict the EV-HRG model calculations using the fugacity expansion (21), truncated at the second (dashed blue line), third (dash-dotted red line), and fourth (dotted black line) orders. Lattice QCD data from Refs. [10] and [34,67] are depicted, respectively, by open and full symbols.

of the $\chi_2^B - \chi_4^B$ difference were suggested as a possible indicator of deconfinement in [68], our analysis suggests an alternative possibility in terms of repulsive baryonic interactions. The model predictions are no longer consistent with the lattice data at $T > 185$ MeV. For example, it was checked that χ_4^B becomes negative at $T \simeq 187$ MeV, a behavior not seen in lattice simulations.

The success of the EV-HRG model in describing the Fourier coefficients and the baryon number susceptibilities does not automatically mean that such a model describes all other QCD observables, for instance the correlations and fluctuations involving the electric charge and strangeness, in the same temperature range. These observables are sensitive to the baryon–baryon interactions as well [11]. At the same time, they are also sensitive to interactions involving mesons, as these carry both electric charge and strangeness, and to the strangeness-dependent baryonic interactions [62,69]. These extensions are beyond the scope of the present paper.

5.2. Parameters extracted from lattice

We consider a modification of the EV-HRG model, where the first two Fourier coefficients, i.e. the partial pressures from the $|B| = 1$ and $|B| = 2$ sectors, are treated as temperature dependent free parameters, and are fitted to the lattice data. This corresponds to calculating the functions $\phi_B(T)$ and $b(T)$, defined by:

$$\phi_B(T) = \frac{b_1(T)}{2} T^3, \tag{22}$$

and

$$b(T) = -\frac{b_2(T)}{[b_1(T)]^2}\,\frac{1}{T^3}, \tag{23}$$

where $b_1(T)$ and $b_2(T)$ are taken from lattice simulations. These relations follow from Eqs. (13) and (14). The lattice-extracted $b(T)$ is plotted in Fig. 3.

The values of $b(T)$ are fairly consistent with 1 fm^3 at $T <$ 190 MeV. It is interesting that $b(T)$ shows plateau slightly above the pseudocritical temperature. $b(T)$ monotonously decreases at high temperatures, in the regions where one does not expect to find hadrons in their normal form. In fact, to reproduce the asymptotic expectation of the $b_k/(b_1)^k$ ratios being independent of temperature, the parameter b has to scale as $b \propto 1/T^3$ at high temperatures.

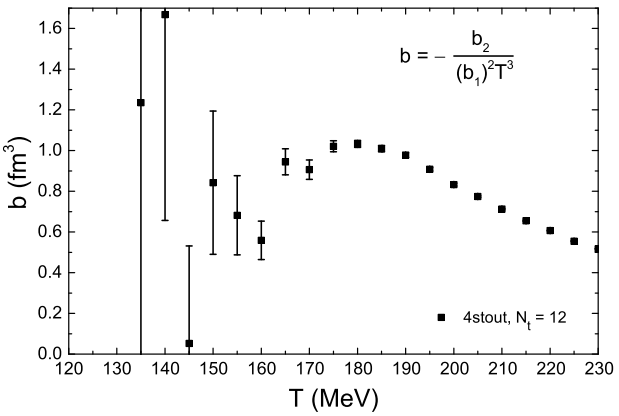


Fig. 3. The temperature dependence of the "eigenvolume parameter" $b(T)$, as estimated from the lattice according to Eq. (23).

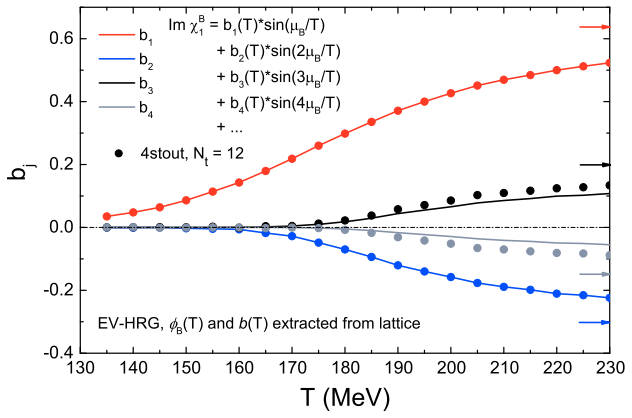


Fig. 4. Same as Fig. 1, but calculated for the modified EV-HRG model, where the first two Fourier coefficients are not taken from standard EV-HRG, but are tuned to exactly reproduce the lattice data by construction, using Eqs. (22) and (23), and the higher coefficients are calculated from these b_1 and b_2 using the formulas given by the EV-HRG model.

Of course, the estimate plotted in Fig. 3 is only a model-dependent interpretation of the lattice data, which should be treated with care. This scenario corresponds to a hadronic description with eigenvolume interactions for baryon–baryon and for antibaryon–antibaryon pairs, while all other hadron pairs are considered to be non-interacting. In general, even for the purely hadronic description, the $b(T)$ values extracted from the lattice reflect the net contribution to the 2nd virial coefficient of both the repulsive and the attractive baryonic interactions. This contribution is averaged over all baryon–baryon pairs. Thus, it cannot distinguish possible differences in virial coefficients for different baryon pairs, for instance involving the strange baryons [69]. If the attractive interactions are non-negligible, then $b(T)$ cannot be attributed exclusively to the baryonic eigenvolume. Since the nucleon–nucleon interaction is attractive at the intermediate range, it is predicted that $b(T)$ should become negative at sufficiently small temperatures, where the hadron gas is dilute and where the average distance between baryons becomes larger.

At high temperatures, $T > 185$ MeV, the lattice data for the b_1 coefficient cannot be described by the standard baryonic spectrum in HRG, as seen from Fig. 1. The function ϕ_B, as extracted from the lattice with Eq. (22), no longer reflects baryons in their normal vacuum form. Nevertheless, it is interesting that the EV-HRG model with the lattice-extracted $\phi_B(T)$ and $b(T)$ gives a reasonable description of the b_3 and b_4 coefficients even at temperatures $T > 200$ MeV (Fig. 4). This is quite notable since the b_3 and b_4 coefficients are not used to extract $\phi_B(T)$ and $b(T)$ from the lattice. One can expect a similar picture for the higher order coefficients, which define the properties of the more and more dense baryon medium. The result suggests that the EV-HRG model has a certain predictive power, particularly regarding the baryon-rich region of the phase diagram, which is presently unaccessible by the lattice simulations. These questions will be explored in the future studies.

6. Summary

We presented the lattice QCD observables at an imaginary baryochemical potential, and analyzed them in the framework of a hadron resonance gas model with repulsive interactions between baryons. More specifically, the temperature dependent Fourier coefficients of the Fourier series expansion of the net baryon density at imaginary μ_B were considered. The ideal hadron resonance gas model predicts zero values for the 2nd and higher-order coefficients. Thus, significant deviations from zero of the higher-order coefficients signal the end of the applicability of the ideal HRG model. Lattice calculations predict that the onset of this behavior takes place at about $T = 160$ MeV. They also predict an alternating sign structure for the coefficients: the odd order coefficients, b_1 and b_3 are positive, while the even order ones, b_2 and b_4, are negative.

Remarkably, the behavior of the first four Fourier coefficients at $T \lesssim 185$ MeV appears to be well described by the HRG model with the excluded-volume interactions between baryons, characterized by a single eigenvolume parameter $b \simeq 1$ fm^3. We do note that some finer structures, such as the temperature derivatives of the coefficients, or the difference $\chi_2^B - \chi_4^B$ of baryon number susceptibilities at $\mu_B = 0$, are reproduced by this simple model only up to a lower temperature of about 175 MeV. The EV-HRG model also predicts the alternating sign structure analytically. At the same time, the van der Waals HRG model, with vdW parameters a and b fixed by the properties of the nuclear ground state, does a worse job in describing the Fourier coefficients. It will be interesting to reconcile these two approaches in order to obtain a unified model for the hadronic equation of state. This model would describe both, the nuclear matter properties at low temperatures and high baryon densities, and the lattice QCD data at high temperatures. A proper hadronic baseline is crucially important for the ongoing experimental effort in determining the properties of QCD from the heavy-ion collision experiments at different collision energies.

The present study elucidates the potential of the lattice QCD observables at imaginary chemical potentials to shed light on the properties of QCD, particularly regarding the hadronic interactions in the confined phase. Such analysis should also be performed for other imaginary μ observables, e.g. involving the electric charge and strangeness, as well as for the more accurate, and continuum extrapolated lattice data, which will be available in the future.[4]

Acknowledgements

We are grateful to Szabolcs Borsányi for stimulating discussions and for his help with the lattice data. This work was supported by HIC for FAIR within the LOEWE program of the State of Hesse. V.V. acknowledges the support from HGS-HIRe for FAIR. H.St. acknowledges the support through the Judah M. Eisenberg Laureatus Chair at Goethe University. This project was funded by the DFG

[4] In the final stages of preparation of this paper, Ref. [62] appeared on arXiv. That paper covers a similar topic, but with a different method. Instead of imaginary μ, the $\mu = 0$ simulations are used there, and, unlike present work, only the first b_2 correction to the ideal HRG model is considered in [62].

grant SFB/TR55. This research used resources of the Argonne Leadership Computing Facility, which is a DOE Office of Science User Facility supported under Contract DEAC02-06CH11357. The authors gratefully acknowledge the Gauss Centre for Supercomputing (GCS) for providing computing time for a GCS Large-Scale Project on the GCS share of the supercomputer JUQUEEN [70] at Jülich Supercomputing Centre (JSC), and at HazelHen supercomputer at HLRS, Stuttgart.

Appendix A

This appendix presents the calculation of the Fourier coefficients $b_k(T)$ in the Fourier expansion of the net baryon susceptibility χ_1^B at an imaginary baryochemical potential (4) for the vdW-HRG model [11]. In the vdW-HRG model, the attractive and repulsive baryonic interactions are described by the van der Waals equation, with common a and b parameters for all baryons. For $a = 0$ this model reduces to the EV-HRG model in Sec. 3.2.

Following results of Ref. [11], in the Boltzmann approximation one has the following transcendental equations for $n_B^{\rm vdw}$ and $n_{\bar{B}}^{\rm vdw}$

$$n_B^{\rm vdw} = (1 - b\, n_B^{\rm vdw})\, \lambda_B\, \phi_B(T)\, \exp\left(-\frac{b\, n_B^{\rm vdw}}{1 - b\, n_B^{\rm vdw}}\right) \times \exp\left(\frac{2\, a\, n_B^{\rm vdw}}{T}\right), \tag{24}$$

$$n_{\bar{B}}^{\rm vdw} = (1 - b\, n_{\bar{B}}^{\rm vdw})\, \lambda_B^{-1}\, \phi_B(T)\, \exp\left(-\frac{b\, n_{\bar{B}}^{\rm vdw}}{1 - b\, n_{\bar{B}}^{\rm vdw}}\right) \times \exp\left(\frac{2\, a\, n_{\bar{B}}^{\rm vdw}}{T}\right). \tag{25}$$

The calculation of the coefficients $b_k^{\rm vdw}$ proceeds in essentially the same way as it was done for the EV-HRG model. One assumes the fugacity expansions for $n_{B(\bar{B})}^{\rm vdw}$ in the form (11)–(12), and calculates the $b_k^{\rm vdw}$ by plugging in the fugacity expansion into Eq. (24). The result is

$$b_1^{\rm vdw}(T) = 2\, \frac{\phi_B(T)}{T^3}, \tag{26}$$

$$b_2^{\rm vdw}(T) = -4\, \left(b - \frac{a}{T}\right)\, \phi_B(T)\, \frac{\phi_B(T)}{T^3}, \tag{27}$$

$$b_3^{\rm vdw}(T) = 9\, \left(b^2 - \frac{8}{3}\, \frac{a\, b}{T} + \frac{4}{3}\, \frac{a^2}{T^2}\right)\, [\phi_B(T)]^2\, \frac{\phi_B(T)}{T^3}, \tag{28}$$

$$b_4^{\rm vdw}(T) = -\frac{64}{3}\, \left(b^3 - \frac{39}{8}\, \frac{a\, b^2}{T} + 6\, \frac{a^2\, b}{T^2} - 2\, \frac{a^3}{T^3}\right) \times [\phi_B(T)]^3\, \frac{\phi_B(T)}{T^3}. \tag{29}$$

References

[1] S. Borsanyi, G. Endrodi, Z. Fodor, A. Jakovac, S.D. Katz, S. Krieg, C. Ratti, K.K. Szabo, J. High Energy Phys. 1011 (2010) 077, arXiv:1007.2580 [hep-lat].
[2] S. Borsanyi, Z. Fodor, C. Hoelbling, S.D. Katz, S. Krieg, K.K. Szabo, Phys. Lett. B 730 (2014) 99, arXiv:1309.5258 [hep-lat].
[3] A. Bazavov, et al., HotQCD Collaboration, Phys. Rev. D 90 (2014) 094503, arXiv:1407.6387 [hep-lat].
[4] Y. Aoki, G. Endrodi, Z. Fodor, S.D. Katz, K.K. Szabo, Nature 443 (2006) 675, arXiv:hep-lat/0611014.
[5] S. Borsanyi, et al., Wuppertal-Budapest Collaboration, J. High Energy Phys. 1009 (2010) 073, arXiv:1005.3508 [hep-lat].
[6] A. Bazavov, et al., Phys. Rev. D 85 (2012) 054503, arXiv:1111.1710 [hep-lat].
[7] R. Bellwied, S. Borsanyi, Z. Fodor, S.D. Katz, C. Ratti, Phys. Rev. Lett. 111 (2013) 202302, arXiv:1305.6297 [hep-lat].
[8] S. Borsanyi, Z. Fodor, S.D. Katz, S. Krieg, C. Ratti, K. Szabo, J. High Energy Phys. 1201 (2012) 138, arXiv:1112.4416 [hep-lat].
[9] A. Bazavov, et al., HotQCD Collaboration, Phys. Rev. D 86 (2012) 034509, arXiv:1203.0784 [hep-lat].
[10] R. Bellwied, S. Borsanyi, Z. Fodor, S.D. Katz, A. Pasztor, C. Ratti, K.K. Szabo, Phys. Rev. D 92 (2015) 114505, arXiv:1507.04627 [hep-lat].
[11] V. Vovchenko, M.I. Gorenstein, H. Stoecker, Phys. Rev. Lett. 118 (2017) 182301, arXiv:1609.03975 [hep-ph].
[12] V. Vovchenko, Phys. Rev. C 96 (2017) 015206, arXiv:1701.06524 [nucl-th].
[13] P. Alba, W. Alberico, R. Bellwied, M. Bluhm, V. Mantovani Sarti, M. Nahrgang, C. Ratti, Phys. Lett. B 738 (2014) 305, arXiv:1403.4903 [hep-ph].
[14] P. Alba, R. Bellwied, M. Bluhm, V. Mantovani Sarti, M. Nahrgang, C. Ratti, Phys. Rev. C 92 (2015) 064910, arXiv:1504.03262 [hep-ph].
[15] I.M. Barbour, S.E. Morrison, E.G. Klepfish, J.B. Kogut, M.P. Lombardo, Nucl. Phys. A, Proc. Suppl. 60 (1998) 220, arXiv:hep-lat/9705042.
[16] Z. Fodor, S.D. Katz, Phys. Lett. B 534 (2002) 87, arXiv:hep-lat/0104001.
[17] Z. Fodor, S.D. Katz, J. High Energy Phys. 0203 (2002) 014, arXiv:hep-lat/0106002.
[18] F. Csikor, G.I. Egri, Z. Fodor, S.D. Katz, K.K. Szabo, A.I. Toth, Nucl. Phys., Proc. Suppl. 119 (2003) 547, arXiv:hep-lat/0209114.
[19] C.R. Allton, S. Ejiri, S.J. Hands, O. Kaczmarek, F. Karsch, E. Laermann, C. Schmidt, L. Scorzato, Phys. Rev. D 66 (2002) 074507, arXiv:hep-lat/0204010.
[20] C.R. Allton, M. Doring, S. Ejiri, S.J. Hands, O. Kaczmarek, F. Karsch, E. Laermann, K. Redlich, Phys. Rev. D 71 (2005) 054508, arXiv:hep-lat/0501030.
[21] R.V. Gavai, S. Gupta, Phys. Rev. D 78 (2008) 114503, arXiv:0806.2233 [hep-lat].
[22] S. Basak, et al., MILC Collaboration, in: PoS LATTICE, vol. 2008, 2008, p. 171, arXiv:0910.0276 [hep-lat].
[23] P. de Forcrand, O. Philipsen, Nucl. Phys. B 642 (2002) 290, arXiv:hep-lat/0205016.
[24] M. D'Elia, M.P. Lombardo, Phys. Rev. D 67 (2003) 014505, arXiv:hep-lat/0209146.
[25] L.K. Wu, X.Q. Luo, H.S. Chen, Phys. Rev. D 76 (2007) 034505, arXiv:hep-lat/0611035.
[26] P. de Forcrand, O. Philipsen, J. High Energy Phys. 0811 (2008) 012, arXiv:0808.1096 [hep-lat].
[27] M. D'Elia, F. Sanfilippo, Phys. Rev. D 80 (2009) 014502, arXiv:0904.1400 [hep-lat].
[28] O. Philipsen, C. Pinke, Phys. Rev. D 89 (2014) 094504, arXiv:1402.0838 [hep-lat].
[29] C. Czaban, F. Cuteri, O. Philipsen, C. Pinke, A. Sciarra, Phys. Rev. D 93 (2016) 054507, arXiv:1512.07180 [hep-lat].
[30] M. D'Elia, G. Gagliardi, F. Sanfilippo, Phys. Rev. D 95 (2017) 094503, arXiv:1611.08285 [hep-lat].
[31] P. Alba, et al., Phys. Rev. D 96 (2017) 034517, arXiv:1702.01113 [hep-lat].
[32] R. Bellwied, S. Borsanyi, Z. Fodor, J. Günther, S.D. Katz, C. Ratti, K.K. Szabo, Phys. Lett. B 751 (2015) 559, arXiv:1507.07510 [hep-lat].
[33] J. Gunther, R. Bellwied, S. Borsanyi, Z. Fodor, S.D. Katz, A. Pasztor, C. Ratti, EPJ Web Conf. 137 (2017) 07008, arXiv:1607.02493 [hep-lat].
[34] A. Bazavov, et al., Phys. Rev. D 95 (2017) 054504, arXiv:1701.04325 [hep-lat].
[35] S. Borsányi, et al., Wuppertal-Budapest Collaboration, Talk at Quark Matter 2017 Conference, 5–11 February 2017, Chicago, USA.
[36] M. Bluhm, B. Kampfer, Phys. Rev. D 77 (2008) 034004, arXiv:0711.0590 [hep-ph].
[37] K. Morita, V. Skokov, B. Friman, K. Redlich, Phys. Rev. D 84 (2011) 074020, arXiv:1108.0735 [hep-ph].
[38] M. D'Elia, M.P. Lombardo, Phys. Rev. D 70 (2004) 074509, arXiv:hep-lat/0406012.
[39] M.P. Lombardo, PoS CPOD 2006 (2006) 003, arXiv:hep-lat/0612017.
[40] M. D'Elia, F. Di Renzo, M.P. Lombardo, Phys. Rev. D 76 (2007) 114509, arXiv:0705.3814 [hep-lat].
[41] R. Dashen, S.K. Ma, H.J. Bernstein, Phys. Rev. 187 (1969) 345.
[42] J. Cleymans, H. Satz, Z. Phys. C 57 (1993) 135, arXiv:hep-ph/9207204.
[43] J. Cleymans, K. Redlich, Phys. Rev. Lett. 81 (1998) 5284, arXiv:nucl-th/9808030.
[44] F. Becattini, M. Gazdzicki, A. Keranen, J. Manninen, R. Stock, Phys. Rev. C 69 (2004) 024905, arXiv:hep-ph/0310049.
[45] A. Andronic, P. Braun-Munzinger, J. Stachel, Nucl. Phys. A 772 (2006) 167, arXiv:nucl-th/0511071.
[46] J. Letessier, J. Rafelski, Eur. Phys. J. A 35 (2008) 221, arXiv:nucl-th/0504028.
[47] C. Patrignani, et al., Particle Data Group, Chin. Phys. C 40 (2016) 100001.
[48] F. Becattini, Z. Phys. C 69 (1996) 485.
[49] S. Wheaton, J. Cleymans, M. Hauer, Comput. Phys. Commun. 180 (2009) 84, arXiv:hep-ph/0407174.
[50] L.M. Satarov, V. Vovchenko, P. Alba, M.I. Gorenstein, H. Stoecker, Phys. Rev. C 95 (2017) 024902, arXiv:1610.08753 [nucl-th].
[51] D.H. Rischke, M.I. Gorenstein, H. Stoecker, W. Greiner, Z. Phys. C 51 (1991) 485.
[52] P. Braun-Munzinger, I. Heppe, J. Stachel, Phys. Lett. B 465 (1999) 15, arXiv:nucl-th/9903010.
[53] J. Cleymans, H. Oeschler, K. Redlich, S. Wheaton, Phys. Rev. C 73 (2006) 034905, arXiv:hep-ph/0511094.

[54] J. Randrup, J. Cleymans, Eur. Phys. J. 52 (2016) 218, arXiv:0905.2824 [nucl-th].
[55] A. Andronic, P. Braun-Munzinger, J. Stachel, M. Winn, Phys. Lett. B 718 (2012) 80, arXiv:1201.0693 [nucl-th].
[56] V. Vovchenko, D.V. Anchishkin, M.I. Gorenstein, Phys. Rev. C 91 (2015) 024905, arXiv:1412.5478 [nucl-th].
[57] P. Alba, W.M. Alberico, A. Nada, M. Panero, H. Stöcker, Phys. Rev. D 95 (2017) 094511, arXiv:1611.05872 [hep-lat].
[58] A. Roberge, N. Weiss, Nucl. Phys. B 275 (1986) 734.
[59] S. Borsanyi, et al., Nature 539 (2016) 69, arXiv:1606.07494 [hep-lat].
[60] J. Danzer, C. Gattringer, Phys. Rev. D 86 (2012) 014502, arXiv:1204.1020 [hep-lat].
[61] C. Gattringer, H.P. Schadler, Phys. Rev. D 91 (7) (2015) 074511, arXiv:1411.5133 [hep-lat].
[62] P. Huovinen, P. Petreczky, arXiv:1708.00879 [hep-ph].
[63] J. Takahashi, H. Kouno, M. Yahiro, Phys. Rev. D 91 (1) (2015) 014501, arXiv:1410.7518 [hep-lat].
[64] V.G. Bornyakov, D.L. Boyda, V.A. Goy, A.V. Molochkov, A. Nakamura, A.A. Nikolaev, V.I. Zakharov, Phys. Rev. D 95 (9) (2017) 094506, arXiv:1611.04229 [hep-lat].
[65] D. Boyda, V.G. Bornyakov, V. Goy, A. Molochkov, A. Nakamura, A. Nikolaev, V.I. Zakharov, arXiv:1704.03980 [hep-lat].
[66] E. Beth, G. Uhlenbeck, Physica 4 (1937) 915.
[67] A. Bazavov, et al., HotQCD Collaboration, arXiv:1708.04897 [hep-lat].
[68] A. Bazavov, et al., Phys. Rev. Lett. 111 (2013) 082301, arXiv:1304.7220 [hep-lat].
[69] V. Vovchenko, A. Motornenko, P. Alba, M.I. Gorenstein, L.M. Satarov, H. Stoecker, Phys. Rev. C 96 (2017) 045202, arXiv:1707.09215 [nucl-th].
[70] JUQUEEN, IBM Blue Gene/Q Supercomputer System at the Jülich Supercomputing Centre, Tech. Rep. 1 A1, Jülich Supercomputing Centre, 2015, https://doi.org/10.17815/jlsrf-1-18.